Inorg. Chem. **2002**, *41*, 1855–1861

New Mononuclear, Cyclic Tetranuclear, and 1-D Helical-Chain Cu(II) Complexes Formed by Metal-Assisted Hydrolysis of 3,6-Di-2-pyridyl-1,2,4,5-tetrazine (DPTZ): Crystal Structures and Magnetic Properties

Xian-He Bu,* He Liu, Miao Du, Lei Zhang, and Ya-Mei Guo

Department of Chemistry, Nankai University, Tianjin 300071, People's Republic of China

Mitsuhiko Shionoya

Department of Chemistry, Graduate School of Science, University of Tokyo, Tokyo 113-0033, Japan

Joan Ribas

Department of Chemistry, University of Barcelona, 08028-Barcelona, Spain

Received September 6, 2001

The reactions of 3,6-di-2-pyridyl-1,2,4,5-tetrazine (DPTZ) with different Cu^{II} salts generate two new ligands, 2,5-bis(2-pyridyl)-1,3,4-oxodiazole ($\mathbf{L^1}$) and *N*,*N*′-bis(α-hydroxyl-2-pyridyl)ketazine ($\mathbf{H_2L^2}$), from the metal-assisted hydrolysis of DPTZ, and form three new complexes: a mononuclear complex $[Cu(\mathbf{L^1})_2(H_2O)_2]\cdot 2ClO_4$ (**1**), a linear coordination polymer $[Cu(\mathbf{L^1})(NO_3)_2]_8$ (**2**), and a cyclic tetranuclear complex $[Cu_4(\mathbf{L^2})_2(Im)_2(NO_3)_4(H_2O)_2]$ (**3**) (Im = imidazole). Crystal data for **1**: space group $P2_1/n$ with $a = 10.339(3)$ Å, $b = 10.974(2)$ Å, $c = 13.618(4)$ Å, $\beta = 103.24(1)°$, and $Z = 2$. Crystal data for **2**: space group $C2/c$ with $a = 13.9299(14)$ Å, $b = 9.2275(9)$ Å, $c = 12.1865(13)$ Å, $\beta = 111.248(2)°$, and $Z = 4$. Crystal data for **3**: space group $P2_1/n$ with $a = 9.3422(14)$ Å, $b = 15.987(2)$ Å, $c = 13.963(2)$ Å, $\beta = 108.587(3)°$, and $Z = 2$. $\mathbf{L^1}$ acts as a bidentate chelating ligand in **1** and as a bis-bidentate chelating ligand in **2** with the shortest intramolecular Cu···Cu distance of 6.093 Å. $\mathbf{L^2}$ is a hexadentate ligand to bridge four Cu^{II} ions, forming an interesting neutral cyclic tetranuclear complex **3** with Cu···Cu distances varying from 4.484 to 9.370 Å. The mechanism of the metal assisted hydrolysis of DPTZ is discussed in detail. Magnetic susceptibility measurements indicate that **2** shows weak ferromagnetic interaction ($J = 2.85$ cm^{-1}) along the 1-D helical chain, and that **3** displays weak antiferromagnetic interaction ($J = -1.19$ cm^{-1} for the N—N bridge) and ferromagnetic interaction ($j = 0.11$ cm^{-1} for the O—C═N bridge) between the adjacent Cu^{II} ions.

Introduction

The study of polynuclear transition metal complexes has offered promising perspectives toward developing new functional materials.[1−4] A promising strategy for the construction of polynuclear systems is the hybrid organic/inorganic self-assembly approach in which the inorganic elements are linked by organic bridges, and many excellent examples have been reported.[5−11]

The ligand, 3,6-di-2-pyridyl-1,2,4,5-tetrazine (DPTZ), has been well used as a coordinative π-acceptor moiety of transition metal complexes[12] or as a building block for

* Corresponding author. E-mail: buxh@nankai.edu.cn. Fax: +86-22-23530850.

(1) For examples: (a) Coronado, E.; Delhaes, P.; Gatteschi, D.; Miller, J. S. *Molecular Magnetism: From Molecular Assemblies to the Devices*; Kluwer Academic Publishers: Dordrecht, The Netherlands, 1996. (b) DeMunno, G.; Lloret, F.; Julve, M. In *Magnetism: A Supramolecular Function*; Kahn, O. Ed.; Kluwer Academic Publishers: Dordrecht, The Netherlands, 1996.

(2) For example: *Molecular Nonlinear Optics*; Zyss, J. Ed.; The Academic Press: New York, 1994.

(3) For examples: (a) Feig, A. L.; Lippard, S. J. *Chem. Rev.* **1994**, *94*, 759. (b) Que, L. J.; Dong, Y. *Acc. Chem. Res.* **1996**, *29*, 190. (c) Solomon, E. I.; Brunold, T. C.; Davis, M. I.; Kemsley, J. N.; Lee, S.-K.; Lehnert, N.; Neese, F.; Skulan, A. J.; Yang, Y. S.; Zhou, J. *Chem. Rev.* **2000**, *100*, 235.

(4) For examples: (a) Saito, S.; Yamamoto, Y. *Chem. Rev.* **2000**, *100*, 2901. (b) Luh, T. Y.; Leung, M. K.; Wong, K. T. *Chem. Rev.* **2000**, *100*, 3187. (d) Dong, S. D. *Chem. Rev.* **1998**, *98*, 1997.

10.1021/ic010955y CCC: $22.00
Published on Web 03/01/2002

Chart 1

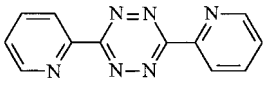

BPTZ

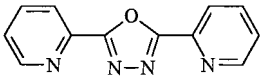

$\mathbf{L^1}$

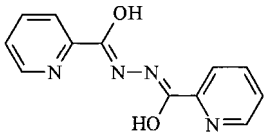

$\mathbf{H_2L^2}$

supramolecular assemblies.[13,14] As a continuation of our interest in the investigation of polynuclear systems, DPTZ was chosen as a bridging ligand to construct novel polynuclear Cu^{II} systems. However, during the course of preparing the Cu^{II} complexes of DPTZ, unexpected hydrolysis reactions took place, two new ligands, 2,5-bis(2-pyridyl)-1,3,4-oxodiazole ($\mathbf{L^1}$) and *N*,*N*′-bis(α-hydroxyl-2- pyridyl)-ketazine ($\mathbf{H_2L^2}$) (see Chart 1), were produced probably through the metal-assisted hydrolysis of DPTZ, and three new Cu^{II} complexes with the two ligands were isolated, a mononuclear complex $[Cu(\mathbf{L^1})_2(H_2O)_2]\cdot 2ClO_4$ (**1**), a 1-D coordination polymer $[Cu(\mathbf{L^1})(NO_3)_2]_8$ (**2**), and a neutral tetranuclear grid complex $[Cu_4(\mathbf{L^2})_2(Im)_2(NO_3)_4(H_2O)_2]$ (**3**) (Im = imidazole), which have been characterized by X-ray diffraction analysis. We report herein the synthesis, characterization, crystal structure, and magnetic properties of these complexes. The influence of the counteranions on the formation of these complexes and the mechanism of the hydrolysis process will also be discussed.

Experimental Section

Materials and General Methods. All the reagents for syntheses were commercially available and used without further purification. Elemental analyses were performed on a Perkin-Elmer 240C analyzer. IR spectra were measured on a FT-IR 170SX (Nicolet) spectrometer with KBr pellets and electronic spectra on a Hitachi UV-3010 spectrometer. The magnetic susceptibilities were measured on polycrystalline samples in 4−300 K temperature range for complexes **2** and **3** with a Quantum Design superconducting SQUID magnetometer. Pascal's constants were used to determine the constituent atom diamagnetism.[15]

Preparation of $[Cu(L^1)_2(H_2O)_2]\cdot 2ClO_4$ (1) and $[Cu(L^1)(NO_3)_2]_8$ (2). Crystals were prepared by layering a solution of $Cu(ClO_4)_2\cdot 6H_2O$ or $Cu(NO_3)_2\cdot 3H_2O$ (0.2 mmol) in CH_3CN (10 mL) upon a solution of DPTZ (0.2 mmol) in $CHCl_3$ (5 mL) in a sealed tube with very careful diffusion. After several days, green cubic crystals of **1** or light blue block crystals of **2** suitable for X-ray analysis were adhered to the wall of the tube. Anal. Calcd for $C_{24}H_{20}N_8O_{12}Cl_2Cu$ (**1**): C, 38.59; H, 2.70; N, 15.00. Found: C, 38.49; H, 2.74; N, 14.89. IR (KBr pellet): 3432bm, 3077m, 1617s, 1556m, 1491s, 1085vs, 1024m, 623m cm^{-1}. Anal. Calcd for $C_{12}H_8N_6O_7Cu$ (**2**): C, 35.00; H, 1.96; N, 20.41. Found: C, 35.20; H, 2.19; N, 20.45. IR (KBr pellet): 3078m, 1619w, 1558m, 1471s, 1425w, 1384vs, 1295s, 1023m, 831m cm^{-1}.

Preparation of $[Cu_4(L^2)_2(Im)_2(NO_3)_4(H_2O)_2]$ (3). To a solution of $Cu(NO_3)_2\cdot 3H_2O$ (48 mg, 0.2 mmol) in CH_3CN (10 mL) was added a solution of DPTZ (24 mg, 0.1 mmol) in $CHCl_3$ (5 mL) to give a green solution. After being stirred for 30 min, a solution of imidazole (7 mg, 0.1 mmol) in $CHCl_3$ (5 mL) was added. Single crystals suitable for X-ray analysis were obtained by very slow evaporation of the solvent. Anal. Calcd for $C_{30}H_{26}N_{16}O_{18}Cu_4$: C, 31.31; H, 2.28; N, 19.48. Found: C, 31.21; H, 2.42; N, 19.05. IR (KBr pellet): 3425b, 3079w, 1628vs, 1518s, 1497m, 1384vs, 1027s, 839m cm^{-1}.

Caution. While we have encountered no problems in handling perchlorate salts in this work, these should be prepared in a small scale and treated with great caution because of the potential explosion.

X-ray Crystallography Studies. Single-crystal X-ray diffraction measurements were carried out on a RAXIS-IV diffractometer (for **1**) or a Bruker Smart 1000 CCD diffractometer (for **2** and **3**) with a graphite-monochromatized Mo Kα radiation (λ = 0.71073 Å). The structures were solved by direct methods and refined on F (for **1**) or F^2 (for **2** and **3**). The non-hydrogen atoms and the hydrogen atoms of **3** were located in successive difference Fourier syntheses, and the hydrogen atoms of **1** and **2** were added theoretically riding on the concerned atoms and refined with fixed thermal factors. The final refinement was performed by full matrix least-squares methods with anisotropic thermal parameters for non-hydrogen atoms. A summary of crystallographic data and experimental details for structural analyses is shown in Table 1.

Results and Discussion

Syntheses and General Characterizations. The reactions of Cu^{II} salts with DPTZ lead to three different nuclearity

(5) For examples: (a) Colacio, E.; Ghazi, M.; Kivekäs, R.; Klinga, M.; Lloret, F.; Moreno, J. M. *Inorg. Chem.* **2000**, *39*, 2770. (b) Gutierrez, L.; Alzuet, G.; Real, J. A.; Cano, J.; Borrás, J.; Castiñeiras, A. *Inorg. Chem.* **2000**, *39*, 3608. (c) Van Albada, G. A.; Mutikainen, I.; Turpeinen, U.; Reedijk, J. *Eur. J. Inorg. Chem.* **1998**, 547.

(6) For examples: (a) Sakiyama, H.; Motoda, K. I.; Okawa, H. *Chem. Lett.* **1991**, 1133. (b) McKee, V.; Tandon, S. S. *Inorg. Chem.* **1989**, *28*, 2901. (c) Zhang, H.; Fu, D.; Ji, F.; Wang, G.; Yu, K.; Yao, T. *J. Chem. Soc., Dalton Trans.* **1996**, 3799.

(7) Tandon, S. S.; Thompson, L. K.; Bridson, J. N. *J. Chem. Soc., Chem. Commun.* **1992**, 911.

(8) Ardizzoia, G. A.; Angaroni, M. A.; La Monica, G.; Cariati, F.; Moret, M.; Masciocchi, N. *J. Chem. Soc., Chem. Commun.* **1990**, 1021.

(9) (a) De Munno, G.; Julve, M.; Lloret, F.; Faus, J.; Verdaguer, M.; Caneschi, A. *Inorg. Chem.* **1995**, *34*, 157. (b) Bu, X. H.; Du, M.; Shang, Z. L.; Zhang, R. H.; Liao, D. Z.; Shionoya, M.; Clifford, T. *Inorg. Chem.* **2000**, *39*, 4190. (c) Castillo, O.; Luque, A.; Sertucha, J.; Roman, P.; Lloret, F. *Inorg. Chem.* **2000**, *39*, 6142.

(10) (a) Deakin, L.; Arif, A. M.; Miller, J. S. *Inorg. Chem.* **1999**, *38*, 5072. (b) Bakalbassis, E.; Bergerat, P.; Kahn, O.; Jeannin, S.; Jeannin, Y.; Dromzee, Y.; Guillot, M. *Inorg. Chem.* **1992**, *31*, 625.

(11) (a) Chui, S. S. Y.; Lo, S. M. F.; Charmant, J. P. H.; Orpen, A. G.; Williams, I. D. *Science* **1999**, *283*, 1148. (b) Noro, S.-I.; Kitagawa, S.; Kondo, M.; Seki, K. *Angew. Chem., Int. Ed.* **2000**, *39*, 2081.

(12) For examples: (a) Roche, S.; Yellowlees, L. J.; Thomas, J. A. *Chem. Commun.* **1998**, 1429. (b) Kaim, W.; Reinhardt, R.; Fieldler, J. *Angew. Chem., Int. Ed. Engl.* **1997**, *36*, 2493 and references therein.

(13) (a) Campos-Fernández, C. S.; Clérac, R.; Dunbar, K. R. *Angew. Chem., Int. Ed.* **1999**, *38*, 3477. (b) Campos-Fernández, C. S.; Clérac, R.; Koomen J. M.; Russell, D. H.; Dunbar, K. R. *J. Am. Chem. Soc.* **2001**, *123*, 773.

(14) Bu, X. H.; Morishta, H.; Tanaka, K.; Biradha, K.; Furusho, S.; Shionoya, M. *Chem. Commun.* **2000**, 971.

(15) *Theory and Application of Molecular Paramagnetism*; Boudreau, E. A.; Mulay, L. N., Eds.; Wiley and Sons: New York, 1976.

Table 1. Crystallographic Data and Structure Refinement Summary for Complexes **1**−**3**

	1	**2**	**3**
formula	$C_{24}H_{20}N_8O_{12}Cl_2Cu$	$C_{12}H_8N_6O_7Cu$	$C_{30}H_{26}N_{16}O_{18}Cu_4$
M_r	746.92	411.78	1150.81
space group	$P2_1/n$	$C2/c$	$P2_1/n$
a/Å	10.339(3)	13.9299(14)	9.3422(14)
b/Å	10.974(2)	9.2275(9)	15.987(2)
c/Å	13.618(4)	12.1865(13)	13.963(2)
β/deg	103.24(1)	111.248(2)	108.587(3)
V/Å^3	1512.7(6)	1459.9(3)	1976.6(5)
D_{calcd} (g cm^{-3})	1.64	1.873	1.933
Z	2	4	2
μ (cm^{-1})	9.74	15.53	22.23
R	0.054	0.0254	0.0374
R_w	0.076	0.0682	0.0800

complexes with different coordination geometry through the metal-assisted hydrolysis of DPTZ. In comparison of **1** with **2**, two different binding modes are found, although the Cu^{II}/DPTZ ratio and the reaction conditions are equal, suggesting that the counteranions have great influence on the structures of the complexes. In fact, anion control has been reported for the coordination polymers of Ag^I with 4,4′-pytz,[16] where the symmetrical structures are strongly dependent upon weak $Ag^I\cdots NO_3^-$ interactions, and in the presence of BF_4^- or PF_6^- anions, the complexes exist as pairs of chains. Therefore, it is no doubt that the counteranion has played an important role for the formation of the two different complexes **1** and **2**. On the other hand, by using the same Cu^{II} salt (for **2** and **3**), the addition of imidazole ligand leads to the formation of an interesting tetranuclear neutral grid complex **3**.

The IR spectra of all three complexes show absorption bands resulting from the skeletal vibrations of the aromatic rings in the 1400−1600 cm^{-1} region. The bands of ClO_4^- appear at 1085 and 623 cm^{-1} for **1**, and the broad bands at ∼3400 cm^{-1} indicate the presence of H_2O. In addition, the spectra of complexes **2** and **3** exhibit strong absorption bands at 1384 and ∼830 cm^{-1} because of the stretch of the NO_3^- anion. The electronic absorption spectra of **1**−**3** in CH_3CN solution display the weak lower energy broad absorption associated with the d−d transition centered at 527 nm for **1**, 516 nm for **2**, and 697 nm for **3**, respectively. The intraligand charge-transfer transitions of the three complexes similarly appear around 280 and 200 nm.

Hydrolysis Reaction of DPTZ. In the previous work,[13,14] no hydrolysis reaction was observed by the reaction of DPTZ ligand with Ni^{II} or Zn^{II}. However, with Cu^{II} salts, the hydrolysis of DPTZ was observed to form two different species in different conditions, which are stabilized by coordination to Cu^{II} under different conditions. A similar Cu^{II}-assisted hydrolysis reaction of 2,4,6-tris(2-pyridyl)-1,3,5-triazine and 2,4,6-tris(2-pyrimidyl)-1,3,5-triazine has been reported.[17] The possible hydrolysis mechanism is postulated

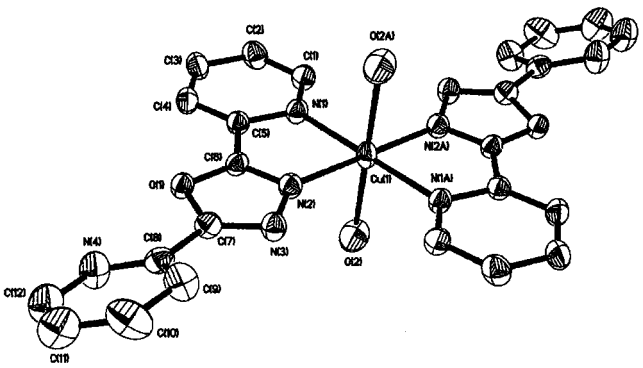

Figure 1. ORTEP view of the complex cation of **1** with 50% thermal ellipsoid probability.

Scheme 1. Possible Mechanism for the Hydrolysis and Complexes Formation Process

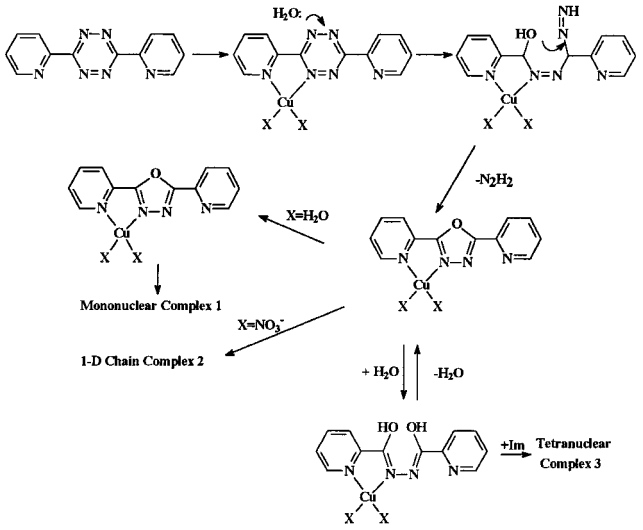

in Scheme 1. The metal ion may promote hydrolysis in two ways: (1) the metal ion acts as a Lewis acid and catalyzes hydrolysis reactions even in neutral solution; (2) the metal ion coordinates to the substrate in such a way as to polarize the chemical bonds, thereby facilitating nucleophilic attack on the reaction center. The carbon center activated by coordination of the imino nitrogen to the Cu^{II} center is very susceptible to nucleophilic attack by H_2O and/or adventitious amounts of H_2O present in the solvent medium. The addition of imidazole (Im) ligand demolished the balance based on $\mathbf{L^1}$, and through exchange reaction with H_2O molecule, promoted the transformation of $\mathbf{L^1}$ to $\mathbf{L^2}$. Unfortunately, our efforts to obtain the product by the reaction of **1** with Im to establish the influence of Im on the hydrolysis and the resulting complex were unsuccessful. Moreover, because other product has not been isolated during the hydrolysis of DPTZ, further investigation on the mechanism is still under way in our lab.

Description of the Crystal Structures. An ORTEP view of $[Cu(\mathbf{L^1})_2(H_2O)_2]\cdot 2ClO_4$ (**1**) including the atomic numbering scheme is shown in Figure 1, and the selected bond distances and angles are given in Table 2. Complex **1** consists of a discrete centrosymmetrical $[Cu(\mathbf{L^1})_2(H_2O)_2]^{2+}$ cation and two ClO_4^- anions. The Cu^{II} ion, which is located at a molecular inversion center, is in an elongated octahedral

(16) Withersby, M. A.; Blake, A. J.; Champness, N. R.; Hubberstey, P.; Li, W. S.; Schröder, M. *Angew. Chem., Int. Ed. Engl.* **1997**, *36*, 2327.
(17) (a) Lerner, E. I.; Lippard, S. J. *J. Am. Chem. Soc.* **1976**, *98*, 5397. (b) Lerner, E. I.; Lippard, S. J. *Inorg. Chem.* **1977**, *16*, 1546. (c) Cantarero, A.; Amigó, J. M.; Faus, J.; Julve, M.; Debaerdemaeker, T. *J. Chem. Soc., Dalton Trans.* **1988**, 2033. (d) Castro, I.; Faus, J.; Julve, M.; Amigó, J. M.; Sletten, J.; Debaerdemaeker, T. *J. Chem. Soc., Dalton Trans.* **1990**, 891.

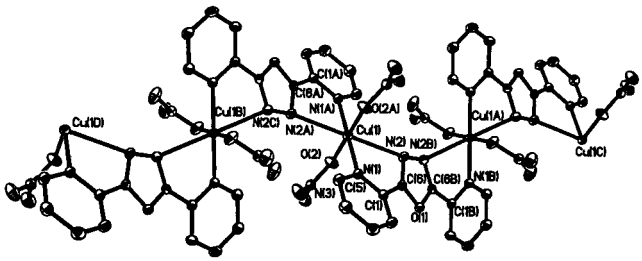

Figure 2. ORTEP view of the linear structure of **2** with 50% thermal ellipsoid probability.

Table 2. Selected Bond Lengths (Å) and Angles (deg) for Complex **1**

Cu(1)−N(1)	2.051(5)	Cu(1)−O(2)	2.336(6)
Cu(1)−N(2)	1.991(4)		
O(2)−Cu(1)−N(1)	87.4(3)	N(1)−Cu(1)−N(2)	81.1(2)
O(2)−Cu(1)−N(2)	89.1(4)		

Table 3. Selected Bond Lengths (Å) and Angles (deg) for Complex **2**

Cu(1)−N(1)	1.9951(15)	Cu(1)−O(2)	1.9804(14)
Cu(1)−N(2)	2.571(6)	Cu(1)···Cu(1A)	6.093
O(2)−Cu(1)−N(1)	94.40(7)	N(1)−Cu(1)−N(2)	75.34(8)
O(2)−Cu(1)−N(2)	82.56(5)		

environment with two H_2O molecules occupying the axial positions. $\mathbf{L^1}$ only uses two of its six potential nitrogen donor atoms, acting as a typical bidentate chelating ligand to form a five-membered Cu−N−C−C−N metallacycle with a N(1)−Cu(1)−N(2) angle of 81.1(2)°. Four Cu−N bond distances vary from 1.991(4) to 2.051(5) Å, and the Cu−O distances involving the water molecules [Cu(1)−O(2) 2.336(6) Å] are longer than those found in the equatorial plane,[18] probably because of the Jahn−Teller effect or drawing by the hydrogen bonds between ClO_4^- and H_2O. There are two noncoordinating ClO_4^- counteranions attached to the complex via hydrogen bonds with the coordinated H_2O. The O···O and H···O separations are 2.996 and 1.883 Å, respectively, falling into the normal range of such separations,[19] and the O−H···O bond angle is 170.4°.

An ORTEP view of the infinite helical chain structure of $[Cu\mathbf{L^1}(NO_3)_2]_8$ (**2**) is shown in Figure 2, and the selected bond distances and angles are given in Table 3. Compound **2** is a neutral polymeric molecule, and the Cu^{II} ions are also six-coordinated with distorted octahedral geometry with two axial positions occupied by the nitrogen atoms of two oxodiazole rings. The Cu−N distances in the axis (2.571 Å) are rather longer than those in the equatorial plane (1.9951(15) Å), indicating a weaker coordination between the Cu^{II} center and the N atoms of the oxodiazole rings probably because of the Jahn−Teller effect. The Cu−O distances (with the nitrate anions) are 1.9804(14) Å, and each $\mathbf{L^1}$ displays a bis-bidentate chelating mode to bridge the metal centers with a shortest intramolecular Cu···Cu separation of 6.093 Å.

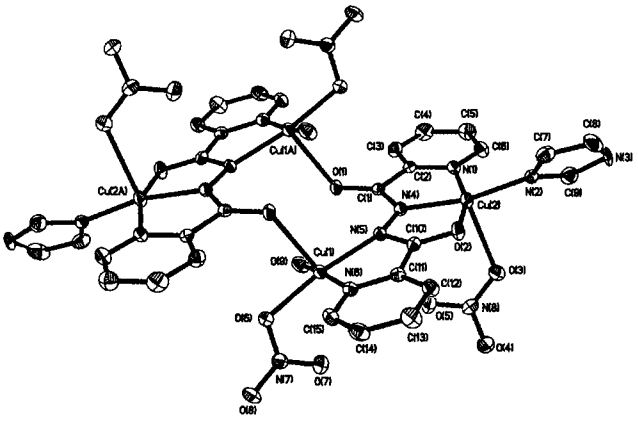

Figure 3. ORTEP view of **3** with 50% thermal ellipsoid probability.

Table 4. Selected Bond Lengths (Å) and Angles (deg) for Complex **3**

Cu(1)−O(9)	1.927(3)	Cu(2)−N(4)	1.924(3)
Cu(1)−N(6)	1.987(3)	Cu(2)−O(2)	1.962(3)
Cu(1)−O(6)	2.010(3)	Cu(2)−N(2)	1.980(3)
Cu(1)−N(5)	2.011(3)	Cu(2)−N(1)	2.022(3)
Cu(1)−O(1A)	2.345(3)	Cu(2)−O(3)	2.409(3)
O(9)−Cu(1)−N(6)	169.74(16)	N(4)−Cu(2)−O(2)	81.14(12)
O(9)−Cu(1)−O(6)	89.41(15)	N(4)−Cu(2)−N(2)	163.66(14)
N(6)−Cu(1)−O(6)	91.45(13)	O(2)−Cu(2)−N(2)	93.47(12)
O(9)−Cu(1)−N(5)	95.97(16)	N(4)−Cu(2)−N(1)	81.40(13)
N(6)−Cu(1)−N(5)	81.96(13)	O(2)−Cu(2)−N(1)	161.64(12)
O(6)−Cu(1)−N(5)	170.93(12)	N(2)−Cu(2)−N(1)	101.79(13)
O(9)−Cu(1)−O(1A)	97.03(14)	N(4)−Cu(2)−O(3)	103.64(12)
N(6)−Cu(1)−O(1A)	93.23(12)	O(2)−Cu(2)−O(3)	86.78(11)
O(6)−Cu(1)−O(1A)	86.74(11)	N(2)−Cu(2)−O(3)	91.36(12)
N(5)−Cu(1)-O(1A)	99.79(11)	N(1)−Cu(2)−O(3)	102.84(12)

The two pyridine rings of $\mathbf{L^1}$ oriented up and down from the oxodiazole ring to form a dihedral angle of 22.5° in **2**. However, in **1**, the coordinated oxodiazole and pyridine ring are almost parallel (the dihedral angle between them is 1.1°). The strong distortion of $\mathbf{L^1}$ in **2** enables the ligand to coordinate to two Cu^{II} ions to form an infinite chain structure.

The ORTEP structure of $[Cu_4(\mathbf{L^2})_2(Im)_2(NO_3)_4(H_2O)_2]$ (**3**) with atom labeling is shown in Figure 3, and the selected bond distances and angles are listed in Table 4. Complex **3** is a cyclic tetranuclear neutral molecule because of the coordinated nitrates and two deprotonated $\mathbf{H_2L^2}$ moieties. The four square-pyramidal Cu^{II} ions are arranged symmetrically in a quadrilateral, in which two Cu^{II} ions (Cu(1) and Cu(1A)) are bridged alternately by the alkoxide oxygen, carbon atoms, and diazine groups of two different ligands to form a ring structure related by a C_2 symmetry, and the other two Cu^{II} ions (Cu(2) and Cu(2A)) are out of the grid. Cu(1) and Cu(2) are pentacoordinated with a different coordination mode. The Cu−N and Cu−O bond distances in the basal plane are almost equivalent (from 1.924(3) to 2.022(3) Å), and the axial Cu−O bonds are 2.339(3) and 2.409(3) Å, respectively, being longer than others in the basal planes. Two nitrogen atoms (N(4) and N(5)) and the alkoxide oxygen atom (O(2)) in one $\mathbf{L^2}$ are located below the Cu_2O_2 plane. In contrast, the two corresponding nitrogen atoms (N(4A) and N(5A)) and oxygen atom (O(2A)) in another $\mathbf{L^2}$ are located above the plane in a chairlike arrangement. The C=N and N−N bond distances are 1.315(3) and 1.398(4) Å, respectively, being consistent with a similar compound

(18) (a) Santis, G. D.; Fabbrizzi, L.; Licchelli, M.; Pallavicini, P. *Coord. Chem. Rev.* **1992**, *120*, 237 and references therein. (b) Bu, X. H.; An, D. L.; Cao, X. C.; Zhang, R. H.; Clifford, T.; Kimura, E. *J. Chem. Soc., Dalton Trans.* **1998**, 2248.

(19) Stout, G. H.; Jensen, L. H. *X-ray Structure Determination*: *A Practical Guide*; MacMillan: New York, 1968.

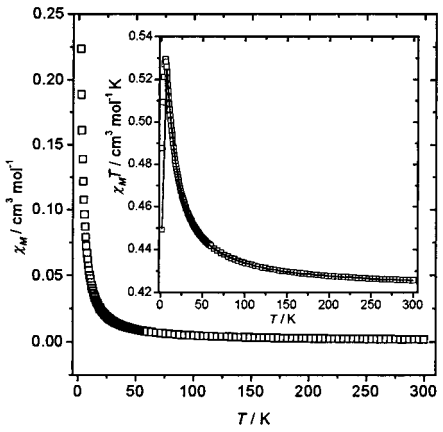

(a)

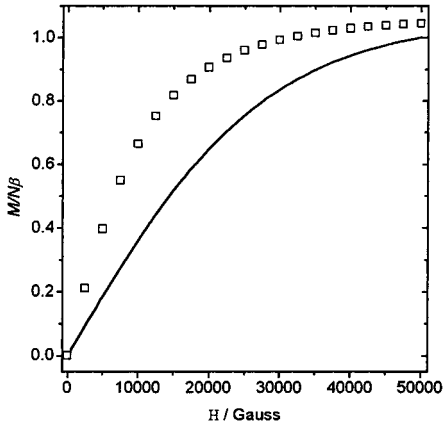

(b)

Figure 4. (a) Thermal variation of the molar magnetic susceptibility, χ_M and $\chi_M T$ product (insert) of **2**. Solid line shows the best fit to the model (see text). (b) Reduced magnetization versus magnetic field for **2** at 2 K. Dotted points are the experimental values; solid line represents the Brillouin function for an $S = {}^1/_2$ spin state with $g = 2.12$.

POAP.[20] These results suggest that $\mathbf{L^2}$ containing the saturated diazine N_2 fragment favors acting as a flexible bridging ligand.[21]

Magnetic Behavior. The temperature (T) dependence of the molecular magnetic susceptibility (χ_M) of **2** is shown in Figure 4a as a plot of χ_M and $\chi_M T$ versus T. χ_M (per Cu ion) increases from 0.0014 $cm^3\ mol^{-1}$ at 300 K to 0.22 $cm^3\ mol^{-1}$ at 2 K. The value of $\chi_M T$ increases from 0.425 $cm^3\ mol^{-1}$ K at 300 K to 0.53 $cm^3\ mol^{-1}$ K at 5 K and then decreases to 0.45 $cm^3\ mol^{-1}$ K at 2 K. The $\chi_M T$ at 300 K is a typical value calculated from an isolated Cu^{II} ion with $g = 2.12$. The shape of this $\chi_M T$ curve is indicative of weak ferromagnetic coupling with an antiferromagnetic coupling acting at low temperatures. The magnetization curve at 2 K up to 50000 G is shown in Figure 4b. The value of the reduced magnetization at 50000 G is 1.05 electrons, clearly indicating that it is close to the saturation value for an unpaired electron with $g > 2.00$.

The magnetic behavior of **2** has been analyzed with a theoretical expression taking into account the intramolecular magnetic interactions between Cu^{II} ions. The spin Hamiltonian appropriate to this system is given in eq 1, where all symbols have their usual meanings.

$$H = -\Sigma J_{ij} S_i S_j \tag{1}$$

The expression of the molecular susceptibility is given in eqs 2−5 for the chain of spins with $S = {}^1/_2$ metal centers.[22]

$$\chi = \frac{Ng^2\beta^2}{4KT}\left[\frac{A}{B}\right]^{2/3} \tag{2}$$

$$A = 1.0 + 5.7979916y + 16.902653y^2 + 29.376885y^3 + 29.832959y^4 + 14.036918y^5 \tag{3}$$

$$B = 1.0 + 2.7979916y + 7.0086780y^2 + 8.653644y^3 + 4.5743114y^4 \tag{4}$$

$$y = J/2KT \tag{5}$$

A molecular field correction has been considered in the mean-field approximation as zj' for interpreting the magnetic interaction between chains.[23]

$$\chi_M = \frac{\chi}{1 - \chi(2zj'/Ng^2\beta^2)} \tag{6}$$

The best fit of the experimental data leads to $J = 2.85$ cm^{-1}, $zj' = -3.05$ cm^{-1}, $g = 2.12$, and $R = 3.01 \times 10^{-5}$ (R is defined as $\Sigma[(\chi_M)_{obs} - (\chi_M)_{calcd}]^2/\Sigma(\chi_M)_{obs}^2$). These results indicate a weak ferromagnetic interaction between Cu^{II} centers via the $\mathbf{L^1}$ bridges. The superexchange pathway that leads to ferromagnetic interaction between Cu^{II} ions is attributed to the apical N−N bridge. Because of the octahedral coordination environments of Cu^{II} centers, the magnetic orbital is described as a $d_{x^2-y^2}$-type, and no spin density is residual on the d_{z^2} orbital. Therefore, the magnetic orbitals are orthogonal which leads to ferromagnetic interaction. On the other hand, the coplanarity of the $\mathbf{L^1}$ ligand is destroyed to bridge the Cu^{II} ions (the dihedral angle between the oxodizole ring and pyridine is 22.5°). The torsion angle Cu−N−N−Cu is rather large (96.4°); that is, the Cu−N−N−Cu is not coplanar, suggesting that the oxodiazole ring does not favor the transfer of magnetic interactions. Similar examples have been observed in the pyrazole-bridged complexes,[24] and the experimental result is in good agreement with the theoretical analysis.

(20) Matthews, C. J.; Avery, K.; Xu, Z.; Thompson, L. K.; Zhao, L.; Miller, D. O.; Biradha, K.; Poirier, K.; Zaworotko, M. J.; Wilson, C.; Goeta, A. E.; Howard, J. A. K. *Inorg. Chem.* **1999**, *38*, 5266.

(21) (a) O'Connor, C. J.; Romananch, R. J.; Robertson, D. M.; Eduok, E. E.; Fronczek, F. R. *Inorg. Chem.* **1983**, *22*, 449. (b) Saroja, J.; Manivannan, V.; Chakraborty, P.; Pal, S. *Inorg. Chem.* **1995**, *34*, 3099.

(22) Baker, G. A.; Rushbrooke, G. S. J.; Gilbert, H. E. *Phys. Rev.* **1964**, *135A*, 1272.

(23) Myers, B. E.; Berger, L.; Friedberg, S. A. *J. Appl. Phys.* **1968**, *40*, 1149.

(24) Xu, Z.; Thompson, L. K. Matthews, C. J.; Miller, D. O.; Goeta, A. E.; Wilson, C.; Howard, J. A. K.; Ohba, M.; Ōkawa, H. *J. Chem. Soc., Dalton Trans.* **2000**, 69 and references therein.

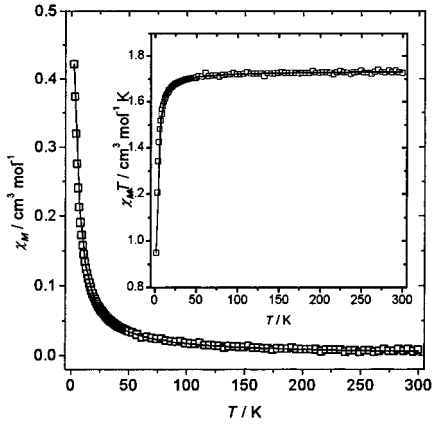

(a)

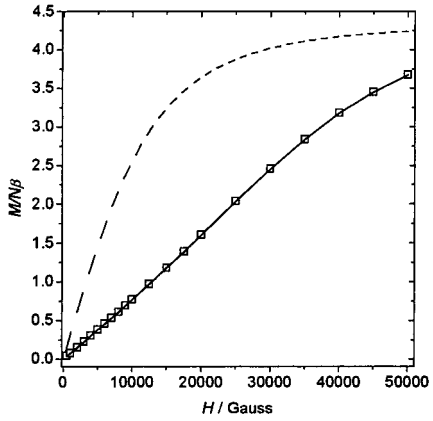

(b)

Figure 5. (a) Thermal variation of the molar magnetic susceptibility, χ_M and $\chi_M T$ product (insert) of **3**. Solid lines show the best fit to the model (see text). (b) Reduced magnetization versus magnetic field for **3** at 2 K. Solid line is the fit for a dinuclear $^1/_2 - {}^1/_2$ complex, scaled by **2** (see text). Dotted points represent the Brillouin function for an $S = 2$ spin state with $g = 2.15$.

The magnetization curve at 2 K does not follow the Brillouin formula for an isolated Cu^{II} ion (Figure 4b). The experimental points lie above the theoretical points, indicating ferromagnetic coupling as shown in the susceptibility calculations. Obviously, at 50000 G, the saturation values must be coincident.

The temperature (T) dependence of the molecular magnetic susceptibility (χ_M) of **3** is shown in Figure 5a as a plot of χ_M and $\chi_M T$ versus T. The value of χ_M (per 4 Cu^{II} ions) increases from 0.008 $cm^3\ mol^{-1}$ at 300 K to 0.42 $cm^3\ mol^{-1}$ at 2 K. $\chi_M T$ is practically constant (1.72−1.73 $cm^3\ mol^{-1}$ K) from 300 to 70 K and then decreases to 0.95 $cm^3\ mol^{-1}$ K at 2 K. The $\chi_M T$ at 300 K is a typical value calculated for four isolated Cu^{II} ions with $g = 2.15$. The shape of this $\chi_M T$ curve is indicative of a global weak antiferromagnetic coupling. The magnetization curve at 2 K up to 50000 G is shown in Figure 5b. The value of the reduced magnetization at 50000 G is 3.68 electrons, lower than the expected value for the saturation for four unpaired electrons with $g > 2.00$ (>4).

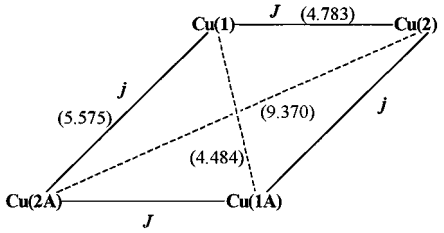

Figure 6. Model of the magnetic exchange interactions in **3** (the Cu···Cu distances (Å) are in parentheses).

This curve does not follow the Brillouin formula, also indicating antiferromagnetic coupling (Figure 5b).

Considering the symmetry of **3**, a topological exchange pathway was proposed to evaluate the magnetic properties (Figure 6). The first exchange interaction, J, involves the two Cu^{II} centers Cu(1) and Cu(2), which are linked by an N−N bridge. The second exchange interaction, j, represents the magnetic interaction bridged by an O−C−N bridge. The spin Hamiltonian is given in eq 7:

$$H = -J(S_1S_2 + S_{1'}S_{2'}) - j(S_1S_{2'} + S_{1'}S_2) \tag{7}$$

The low-lying energy levels shown in eqs 8−13 were deduced using an energy matrix diagonalization method[25] and inserted into the van Vleck equation (eq 14)[26] to give the expression of the molecular susceptibility (eq 15), which was used to fit the experimental data.

$$E_1 = -(J + j) \tag{8}$$

$$E_2 = J - j \tag{9}$$

$$E_3 = j - J \tag{10}$$

$$E_4 = J + j \tag{11}$$

$$E_5 = J + j - 2(J^2 + j^2)^{1/2} \tag{12}$$

$$E_6 = J + j + 2(J^2 + j^2)^{1/2} \tag{13}$$

$$\chi_M = \frac{Ng^2\beta^2}{3KT} \frac{\Sigma_{S_T} S_T(S_T + 1)(2S_T + 1)e^{-E(S_T)/KT}}{\Sigma_{S_T}(2S_T + 1)e^{-E(S_T)/KT}} \tag{14}$$

$$\chi_M = (0.125g^2/T)[30\exp(-E_1/kT) + 6\exp(-E_2/kT) + 6\exp(-E_3/kT) + 6\exp(-E_4/kT)]/[5\exp(-E_1/kT) + 3\exp(-E_2/kT) + 3\exp(-E_3/kT) + 3\exp(-E_4/kT) + \exp(-E_5/kT) + \exp(-E_6/kT)] \tag{15}$$

The solid lines in Figure 5a represent the best fit of the data to eq 15, and the final parameters were $J = -1.19\ cm^{-1}$, $j = 0.11\ cm^{-1}$, $g = 2.15$, and $R = 1.7 \times 10^{-5}$. The negative J value confirms the intramolecular antiferromagnetic interaction. The j value indicates low ferromagnetic coupling between the dinuclear entities. Taking into account the structure and calculated J values, we attempted to fit the

(25) Jotham, R. W.; Kettle, S. F. A. *Inorg. Chim. Acta* **1970**, *4*, 145.
(26) van Vleck, J. H. *The Theory of Electric and Magnetic Susceptibilities*; Oxford University Press: London, 1932.

experimental results as a dinuclear Cu^{II} complex, giving $J_{intra} = -2.30\ cm^{-1}$, $J_{inter} = 0.06\ cm^{-1}$, $g = 2.15$, and $R = 9.5 \times 10^{-5}$. These results are of the same order of magnitude as those calculated for a tetranuclear complex. As indicated previously, the magnetization curve does not follow the Brillouin formula, but the experimental data lie below the theoretical points. If the antiferromagnetic coupling is high, the experimental curve would show points with very low $M/N\beta$ values. The experimental data, close to the theoretical ones, indicate low antiferromagnetic coupling. Considering the magnetization data as a dinuclear complex, it was possible to fit the curve by a full diagonalization method, giving $J = -2.3\ cm^{-1}$ and $g = 2.14$ in very good agreement with the values calculated from the susceptibility curves.

For **3**, the antiferromagnetic interaction is expected for the Cu^{II} centers bridged by *trans*-diazine groups; otherwise, the weakness of the magnetic interaction is unexpected compared with other tetranuclear Cu^{II} complexes. In an earlier study by Thompson,[20,27] the significant antiferromagnetic interaction between Cu^{II} centers is observed because of the effective p orbital arrangement within the N−N bridge. Significant weakness of the magnetic interaction can be understood according to $J_{AF} = -2S(\Delta^2 - \delta^2)$ for noncentrosymmetric binuclear magnetic interaction (Cu(1) and Cu(2)), Δ being the energy separation between the two single occupied molecular orbitals in the triplet state built from the magnetic orbitals and δ being the energy separation between the magnetic orbitals. Because of the lowering of symmetry, the δ value increases which leads to the corresponding decrease in the antiferromagnetic interaction. Furthermore, the deviations of the Cu^{II} ion above the basal plane defined by the group (O1−C1−N4−N5−C10−O2) are 0.128 and 0.542 Å, respectively. The overlap of the magnetic orbitals ($d_{x^2-y^2}$ for Cu^{II} and p for N) was reduced significantly, which leads to the weakness of the magnetic interaction.

(27) (a) Xu, Z.; Thompson, L. K.; Miller, D. O. *Inorg. Chem.* **1997**, *36*, 3985. (b) Thompson, L. K.; Xu, Z.; Goeta, A. E.; Howard, J. A. K.; Clase, H. J.; Miller, D. O. *Inorg. Chem.* **1998**, *37*, 3217. (c) Xu, Z.; Thompson, L. K.; Miller, D. O.; Clase, H. J.; Howard, J. A. K.; Goeta, A. E. *Inorg. Chem.* **1998**, *37*, 3620.

Conclusions

The reactions of Cu^{II} salts with DPTZ generate two new polydentate ligands through the hydrolysis of the DPTZ ligand with the assistance of Cu^{II}. The new ligands coordinate to Cu^{II} ions to form mononuclear, cyclic tetranuclear, and 1-D helical chain complexes in the hydrolysis process, which may be promoted by the addition of imidazole. The X-ray analyses revealed that the coordination modes of Cu^{II} are influenced by the counteranions. Our study indicates that the DPTZ ligand that contains two N═N double bonds is unstable in the presence of Cu^{II} and H_2O.

Weak ferromagnetic behavior of **2** along the diazine bridge is attributed to the favorable orthogonal interaction of the magnetic orbitals of Cu^{II} centers due to the helical arrangement of the chain. This is the first example in which the N−N group of the oxodizole ring bridges Cu^{II} centers on the axial position. Compound **3** shows weak antiferromagnetic interaction between the Cu^{II} centers bridged by the N−N group in a trans mode, caused by the noncentrosymmetric structure and longer distances from the Cu^{II} ions to the bridging plane.

Acknowledgment. This work was financially supported by NSFC (29971019) of China. We thank Dr. M. Shiro for the determination of the crystal structure of **1**. J. Ribas acknowledges the financial support from the Spanish Government (Grant BQU2000-0791).

Supporting Information Available: Three X-ray crystallographic files in CIF format. This material is available free of charge via the Internet at http://pubs.acs.org.

IC010955Y